

# Electric Dipolar Kondo Effect Emerging from Vibrating Magnetic Ion

Takashi Hotta<sup>1</sup> and Kazuo Ueda<sup>2</sup>

<sup>1</sup>*Department of Physics, Tokyo Metropolitan University, Hachioji, Tokyo 192-0397, Japan*

<sup>2</sup>*Institute for Solid State Physics, University of Tokyo, Kashiwa, Chiba 277-8581, Japan*

(Dated: November 25, 2018)

When a magnetic ion vibrates in a metal, it inevitably introduces a new channel of hybridization with conduction electrons and in general, the vibrating ion induces electric dipole moment. In such a situation, we find that magnetic and non-magnetic Kondo effects alternatively occur due to the screening of spin moment and electric dipole moment of vibrating ion. In particular, electric dipolar two-channel Kondo effect is found to occur for weak Coulomb interaction. We also show that magnetically robust heavy-electron state appears near the fixed point of electric dipolar two-channel Kondo effect. We believe that the *vibrating* magnetic ion opens a new door in the Kondo physics.

PACS numbers: 75.20.Hr, 71.27.+a, 75.40.Cx

It has been widely recognized that Kondo phenomena generally appear when localized entity with internal degrees of freedom is coupled with conduction electrons. Concerning the original problem of resistance minimum phenomenon in metals with magnetic impurities, Kondo has actually shown it by quantum-mechanical calculations for scattering amplitude of electrons due to magnetic impurities [1]. Then, it has been revealed that the singlet state is formed from local magnetic moment due to the coupling with conduction electrons [2]. After the understanding of the Kondo effect in the dilute magnetic impurity system, interests of researchers have moved to the impurity with complex degrees of freedom.

One research direction has been found in the explicit consideration of orbital degree of freedom of localized electron. Coqblin and Schrieffer have derived exchange interactions from the multiorbital Anderson model [3]. Then, the concept of multi-channel Kondo effect has been developed on the basis of such exchange interactions [4], as a potential source of non-Fermi liquid phenomena. Such non-Fermi liquid properties have been pointed out also in a two-impurity Kondo system [5, 6]. Concerning the reality of two-channel Kondo effect, Cox has pointed out the existence of two screening channels in the case of quadrupole degree of freedom in a cubic uranium compound with non-Kramers doublet ground state [7].

Another possibility is non-magnetic Kondo effect with phonon origin. First Kondo has considered Kondo-like behavior in a two-level system [8]. The two-level Kondo system has been proven to exhibit the same behavior as the magnetic Kondo effect [9]. Yu and Anderson have discussed the phononic Kondo effect from a different viewpoint [10]. They have pointed out that the scattering process between spinless *s*-wave conduction electron to *p*-wave one is produced by ion displacement.

Recently, the Kondo effect with phonon origin has attracted renewed attention due to active experimental investigations on cage structure materials, in which a guest ion is vibrating in a cage composed of relatively light atoms. We believe that the vibration of magnetic ion in

the cage provides a new ingredient in the Kondo physics, since dynamical aspects of magnetic impurity have been considered unsatisfactorily in the Kondo problem. In fact, quite recently, the two-channel Kondo effect has been confirmed in the model for vibrating magnetic impurity [11–14]. Also for the promotion of our understanding on magnetically robust heavy-electron phenomenon observed in cage compound [15], we further develop the Kondo physics of vibrating magnetic impurity.

In this Letter, we analyze a two-channel conduction electron system hybridized with vibrating magnetic ion by using a numerical renormalization group technique. We confirm magnetic and non-magnetic Kondo effects originating from the screening of spin and electric dipolar moments, respectively, by evaluating entropy and susceptibilities for spin and electric dipole moments. Near the fixed point for electric dipolar two-channel Kondo effect, we find magnetically robust heavy-electron state from the direct evaluation of the Sommerfeld constant.

Let us consider a two-channel conduction electron system hybridized with vibrating magnetic impurity [12–14]. In the unit of  $\hbar=k_B=1$ , the Hamiltonian is given by

$$\begin{aligned}
 H = & \sum_{\mathbf{k},\sigma} \left[ \varepsilon_{\mathbf{k}} (c_{\mathbf{k}s\sigma}^\dagger c_{\mathbf{k}s\sigma} + c_{\mathbf{k}p\sigma}^\dagger c_{\mathbf{k}p\sigma}) \right] \\
 & + \sum_{\mathbf{k},\sigma} \left[ V_0 (c_{\mathbf{k}s\sigma}^\dagger f_\sigma + \text{h.c.}) + g x (c_{\mathbf{k}p\sigma}^\dagger f_\sigma + \text{h.c.}) \right] \quad (1) \\
 & + U n_\uparrow n_\downarrow + E_f (n_\uparrow + n_\downarrow) + \omega x^2/2 + p^2/2,
 \end{aligned}$$

where  $\varepsilon_{\mathbf{k}}$  denotes conduction electron dispersion,  $c_{\mathbf{k}\ell\sigma}$  indicates the annihilation operator for conduction electron with momentum  $\mathbf{k}$ , angular momentum  $\ell$ , and spin  $\sigma$ ,  $f_\sigma$  is the annihilation operator for localized electron with spin  $\sigma$ ,  $n_\sigma = f_\sigma^\dagger f_\sigma$ ,  $U$  is the Coulomb interaction between localized electrons,  $E_f$  denotes the local *f*-level energy,  $V_0$  is the hybridization between *s*-channel conduction and localized *f* electrons,  $g$  is the electron-vibration coupling,  $x$  denotes the ion displacement,  $p$  indicates the corresponding canonical momentum, and  $\omega$  is the vibration frequency. Note that we set the reduced mass of vibra-

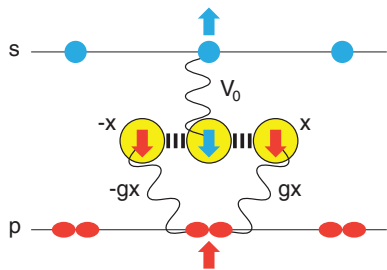


FIG. 1: (Color online) Schematic view of the situation described by the model Hamiltonian (1).

tion as unity. In order to consider the symmetric case, we set  $E_f = -U/2$  throughout this paper.

In this paper, we analyze the model with the use of a numerical renormalization group (NRG) method [16]. We introduce a cut-off  $\Lambda$  for the logarithmic discretization of the conduction band. Due to the limitation of computer resources, we keep  $N$  low-energy states. In this paper, we set  $\Lambda=5$  and  $N=5000\sim 10000$ . Note that the temperature  $T$  is defined as  $T=\Lambda^{-(i-1)/2}$  in the NRG calculation, where  $i$  is the number of the renormalization step. The phonon basis is truncated at a finite number  $N_{\text{ph}}$ , which is set as  $N_{\text{ph}}=300$  in this paper.

It is convenient to introduce phonon operators  $a$  and  $a^\dagger$  through the relation of  $x=(a+a^\dagger)/\sqrt{2\omega}$ . Then, we define the magnitude of phonon-assisted hybridization as  $V_1=g/\sqrt{2\omega}$ . The energy unit is the half of the conduction electron band  $D$ , which is set as unity. As for parameters, we set  $V_0=\omega=0.2$  and we change the values of  $U$  and  $V_1$ .

First let us visualize the situation described by the present model. In Fig. 1, the two horizontal lines symbolically denote  $s$  and  $p$  channels which are hybridized with magnetic impurity. As shown in  $H$ ,  $s$ -channel electrons are hybridized with localized electron in a standard manner, while the hybridization process between  $p$ -channel and localized electrons is assisted by phonons. Note that parities of  $s$ - and  $p$ -channel electrons are different, as easily understood from the values of angular momenta. Namely,  $s$ - and  $p$ -channel electrons possess even and odd parities, respectively. Since the parity for ion displacement  $x$  is odd, it is natural that the phonon-assisted hybridization occurs only for  $p$  channel.

When magnetic ion stops at an origin, we consider only the screening of impurity spin moment by  $s$ -channel electrons, leading to the conventional Kondo effect. However, when the ion is vibrating as shown in Fig. 1, there occurs another screening process due to  $p$ -channel electrons. In such a situation, in addition to the screening of spin moment, the electric dipole moment in proportion to the displacement  $x$  should be also screened by conduction electrons, leading to non-magnetic Kondo effect. Intuitively, we understand that the main screening channel is converted between  $s$  and  $p$  due to the balance between  $V_0$  and  $V_1$ . In fact, the phases with different

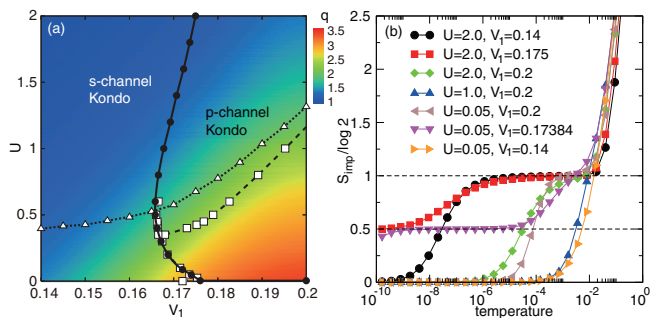


FIG. 2: (Color online) (a) Phase diagram on the  $V_1$ - $U$  plane for  $V_0=\omega=0.2$ . The color gradation indicates the magnitude of average displacement  $q$ . Solid curve with solid circles denote the two-channel Kondo line. Dotted curve with open triangles and broken curve with open squares denote  $d^2q/dU^2=0$  and  $d^2q/dV_1^2=0$ , respectively. As for the definition of  $q$ , see the main text. (b) Entropy vs. temperature.

quantum numbers in relation with parity have been found to be converted between the regions of large and small  $V_1$ . Then, two-channel Kondo effect has been confirmed to occur just at the boundary between those two phases [11–13]. However, another conversion between magnetic and non-magnetic Kondo effects controlled by the balance between  $U$  and  $V_1$  has not been clarified yet. Then, in this paper, we unveil such a new point in relation with magnetically robust heavy electron state.

Now we explain the phase diagram in Fig. 2(a). As mentioned above, the solid curve indicates the boundary between two phases with different quantum numbers, which are obtained by the  $s$ - and  $p$ -channel Kondo screening, respectively. On the boundary curve between two phases, the two-channel Kondo effect is realized. Since no phase conversion occurs on the line of  $U=0$ , the boundary curve asymptotically approaches the line of  $U=0$ . Note that low-energy spectra of three fixed points of  $s$ -channel,  $p$ -channel, and two-channel Kondo states have been revealed in Refs. [12] and [13]. New results of this paper are color gradation and other broken and dotted curves. Their meanings will be discussed later.

Next we discuss the NRG results of entropy. In Fig. 2(b), we show the change of entropy along the lines of  $U=2$ ,  $V_1=0.2$ , and  $U=0.05$ . On the line of  $U=2$ , for  $V_1=0.14$  and  $0.2$ , we find the plateaus of  $\log 2$ , which are eventually released at low enough temperatures. At  $(V_1, U)=(0.175, 2)$ , we observe the entropy of  $0.5 \log 2$  at low temperatures, which is the signal of two-channel Kondo effect. When we decrease the value of  $U$  from  $U=2$  on the line of  $V_1=0.2$ , we observe the increase of the Kondo temperature  $T_K$ , which is characterized by the release of entropy  $\log 2$ . This is quite natural from the viewpoint of the conventional magnetic Kondo effect. Thus, we deduce that the Kondo effect on the line of  $U=2$  as well as in the region of  $U \gtrsim 1$  on the line of  $V_1=0.2$  is originating from the screening of impurity spin moment.

However, for  $U \lesssim 1$ , a plateau of  $\log 2$  again appears. The temperature region of  $\log 2$  is wider for smaller  $U$  and  $T_K$  is decreased with the decrease of  $U$ . Such behavior is contradictory to the conventional magnetic Kondo effect. Furthermore, at  $(V_1, U) = (0.17384, 0.05)$ , we again observe a clear plateau of entropy of  $0.5 \log 2$ , but it is difficult to understand the origin of this two-channel Kondo behavior only from the result of entropy.

In order to clarify what quantity is screened, we evaluate susceptibilities for magnetic and electric dipole moments, which are, respectively, defined by

$$\chi_M = \int_0^{1/T} d\tau \langle M(\tau)M \rangle, \quad \chi_P = \int_0^{1/T} d\tau \langle P(\tau)P \rangle. \quad (2)$$

Here  $\langle \dots \rangle$  denotes the operation to take thermal average,  $M(\tau) = e^{H\tau} M e^{-H\tau}$ ,  $M = g_s \mu_B (n_\uparrow - n_\downarrow)/2$ , and  $P = Ze(a + a^\dagger)/\sqrt{2\omega}$ , where  $g_s$  is the electron  $g$ -factor which is set as  $g_s = 2$ ,  $\mu_B$  is the Bohr magneton,  $Z$  is valence number of ion, and  $e$  is electric charge. In the actual calculations, we normalize them as  $\chi_M/\mu_B^2$  and  $\chi_P/(Z^2 e^2/2\omega)$ .

In Fig. 3(a), we show  $T\chi_M$  for the same values of  $U$  and  $V_1$  in Fig. 2(b). As we have deduced above, on the line of  $U=2$ , we observe the decrease of  $T\chi_M$  around  $T_K$ . Note that the curves of  $T\chi_M$  for  $V_1=0.14$  and  $V_1=0.2$  at  $U=2$  are quite similar at low temperatures, when  $T$  is rescaled by  $T_K$ . On the other hand, the curve of  $T\chi_M$  for  $(V_1, U) = (0.175, 2)$  is apparently different from those for  $V_1=0.14$  and  $V_1=0.2$ . It is due to the non-Fermi liquid behavior in the two-channel Kondo effect, leading to  $\chi_M \sim -\log T$ . This logarithmic correction in  $\chi_M$  is clearly observed. Along the lines of  $V_1=0.2$  and  $U=0.05$ ,  $T\chi_M$  decreases at relatively high temperature, but the release of the entropy does not seem to correspond to the temperature at which  $T\chi_M$  is decreased.

Now we turn our attention to the results for  $T\chi_P$  in Fig. 3(b). The entropy release for  $(V_1, U) = (0.2, 0.05)$  corresponds to the decrease of  $T\chi_P$ , indicating the occurrence of the Kondo effect concerning electric dipole moment. Note that  $\chi_P$  is related to phonon Green's function. In the strong electron-phonon coupling region, the center of oscillation is shifted either right or left, leading to  $\chi_P \propto q^2/T$ , where  $q = \sqrt{(a + a^\dagger)^2}$ . Thus, for small  $U$  and large  $V_1$  region, we expect that  $T\chi_P$  becomes constant at high temperatures, as found in Fig. 3(b).

When  $T$  is decreased,  $T\chi_P$  is decreased from the constant value due to the Kondo screening of electric dipole moment and it eventually goes to zero at  $T=0$ . This can be called the parity Kondo effect, since near degeneracy with different phonon parities characterizes the electric dipole, which is coupled with conduction electron parity, leading to the non-degenerate ground state with fixed total parity. Note that the total parity is specified by 0 or 1, depending on  $U$  and  $V_1$ . At low enough temperatures, we find  $T\chi_P = 2T/\tilde{\omega}_1$ , where  $\tilde{\omega}_1$  is renormalized phonon energy smaller than  $\omega$ . From the local Fermi-liquid theory, we find  $T_K \propto \tilde{\omega}_1$ , but the proportional

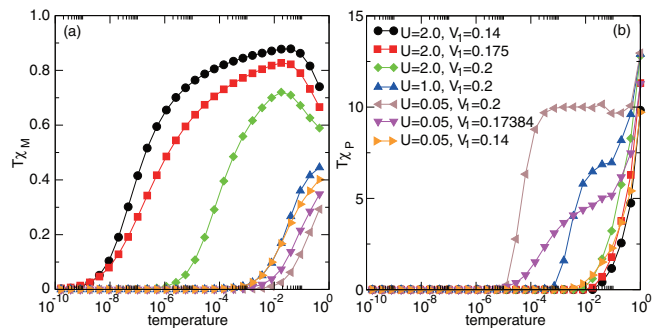


FIG. 3: (Color online) Susceptibilities for (a) magnetic and (b) electric dipole moments as functions of temperature.

coefficient is suppressed by the polaron effect in comparison with the conventional magnetic Kondo effect. Then,  $T\chi_P$  decreases rapidly around  $T_K$  in sharp contrast to  $T\chi_M$  around  $T_K$ . The shape of  $T\chi_P$  at  $(V_1, U) = (0.2, 1.0)$  around  $T_K$  is quite similar to that for  $(0.2, 0.05)$  [17], when  $T$  is rescaled by  $T_K$ . For the case of  $(0.2, 1.0)$ , corresponding to the competing region of magnetic and electric dipolar Kondo effects, we do not find any significant structure in the entropy and  $T\chi_M$ , but in the decrease of  $T\chi_P$  from the shoulder, the enhanced signal can be observed due to the polaron effect in the phonon matrix element of  $\chi_P$ .

We remark that the two-channel Kondo effect also occurs due to the screening of electric dipole moment [18]. In fact, at  $(V_1, U) = (0.17384, 0.05)$ , we find a plateau of entropy  $0.5 \log 2$  and the significant decrease of  $T\chi_P$  around the corresponding temperature. Note that the shape of  $T\chi_P$  at  $(0.17384, 0.05)$  is different from those for  $(0.2, 0.05)$  and  $(0.2, 1.0)$ . We observe the smooth change from  $T\chi_P = \text{constant}$  to  $\chi_P = \text{constant}$  in this case. Since the electric dipole moment is not perfectly screened, vibration still remains and thus, we intuitively obtain  $\chi_P = 2/\tilde{\omega}_2$  in the two-channel electric dipolar Kondo regime, where  $\tilde{\omega}_2$  is another renormalized phonon energy, which is different from  $\tilde{\omega}_1$ . It is one of future tasks to explain the difference between  $\tilde{\omega}_1$  and  $\tilde{\omega}_2$  by overcoming the difficulty to estimate  $\tilde{\omega}_1$  with high precision in the NRG calculation.

Here let us go back to Fig. 1(a). We have found that the electric dipole moment is screened in the region of large  $V_1$  and small  $U$ . In order to visualize the change of the screened moment, we depict  $q$  as the color gradation in Fig. 1(a). For large  $V_1$  and small  $U$ , we find the red region with large  $q$ , in which electric dipolar Kondo effect occurs. On the other hand, there occurs magnetic Kondo effect in the blue region of small  $V_1$  and large  $U$ . As a guide of the boundary between magnetic and non-magnetic Kondo regions, we plot inflection points of  $d^2q/dU^2=0$  (dotted) and  $d^2q/dV_1^2=0$  (broken) in Fig. 1(a). For large  $V_1$ , two curves run in the green area between blue and red regions. Another broken curve

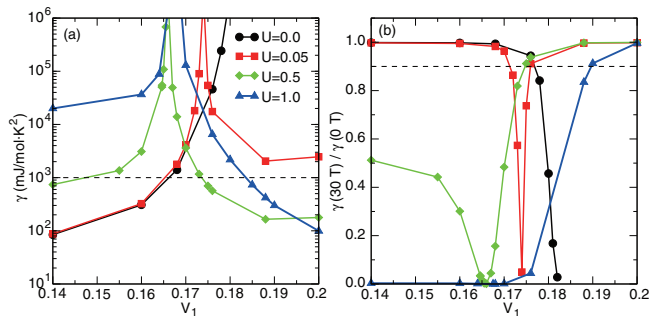


FIG. 4: (Color online) (a) Sommerfeld constant vs.  $V_1$  for  $H=0$  and (b) the ratio of the Sommerfeld constants vs.  $V_1$ .

appears on the two-channel Kondo line for  $U \lesssim 0.6$ , except for  $U=0$ , suggesting the electric dipolar two-channel Kondo region. Note, however, that the inflection points seem to lose the meaning of boundary in the  $s$ -channel Kondo region, since renormalized Fermi chain is realized in the region of small  $U$  and small  $V_1$  [12, 13]. In the small area of yellow and orange of the  $s$ -channel Kondo region, there also occurs non-magnetic Kondo effect, which is interpreted as the Yu-Anderson Kondo effect [10].

Now let us discuss the magnetically robust heavy electron state by the Sommerfeld constant  $\gamma$ . For the purpose, we add the Zeeman term  $H_Z = g_s \mu_B H (n_\uparrow - n_\downarrow)/2$ , where  $H$  is an applied magnetic field, to the model (1). Then, we evaluate  $\gamma$  at  $T = \Lambda^{-14}$ , the lowest temperature at which we can arrive in the present NRG calculations. In Fig. 4(a), we show the results for  $\gamma$  in the unit of  $\text{mJ/mol}\cdot\text{K}^2$  with  $D=1$  eV. We find that  $\gamma$  shows divergent behavior around the two-channel Kondo fixed points, shown by the solid curve in Fig. 1(a). On the line of  $U=0$ , we do not find the phase conversion, but for  $V_1 \gtrsim 0.17$ , the two-channel Kondo line exists in the extreme vicinity of  $U=0$ . Thus,  $\gamma$  becomes very large for  $U=0$  and  $V_1 \gtrsim 0.17$ . In the vicinity of the two-channel Kondo line, we find the enhancement of  $\gamma$  due to the non-Fermi liquid properties, irrespective of  $U$ . For the parameters away from the two-channel Kondo fixed points for  $U > 0.05$ ,  $\gamma$  in the region of the magnetic Kondo effect is relatively large in comparison with that of the non-magnetic Kondo effect of electric dipole moment.

In Fig. 4(b), we show the ratio of  $\gamma$ 's at  $H=0$  T and 30 T. If this ratio is near the unity, we judge that  $\gamma$  is magnetically robust. As we easily imagine, in the Kondo effect concerning the electric dipole moment,  $\gamma$  does not depend sensitively on the magnetic field. As for criteria of the magnetically robust heavy electron state, we consider the conditions of  $\gamma > 1000$  and  $\gamma(30\text{T})/\gamma(0\text{T}) > 0.9$ , shown by horizontal broken lines in Figs. 4(a) and (b). After the NRG calculations, we find that the magnetically robust heavy electron state appears in the region of  $V_1 \gtrsim 0.17$  and  $U \lesssim 0.1$ , except for the narrow region near the two-channel Kondo line. Note that the ratio is strongly suppressed

due to the divergent behavior of  $\gamma(0\text{T})$ . That region is included in the non-magnetic Kondo effect region with orange and red in Fig. 1(a). In comparison with the mechanism of magnetically robust large  $\gamma$  on the basis of the charge Kondo effect [19], it seems to be easier to obtain large  $\gamma$  in the present scenario based on the non-magnetic two-channel Kondo effect.

In summary, we have analyzed the two-channel conduction electron model with vibrating magnetic ion. We have found two types of Kondo effects due to the alternative screening of magnetic and electric dipole moments. Near but not exactly on the two-channel Kondo line with electric dipolar origin, we have found that  $\gamma$  is magnetically robust. Non-magnetic electric dipolar Kondo behavior is expected to be observed in cage-structure materials. In particular, magnetically robust non-Fermi liquid behavior is an interesting possibility.

This work was supported by KAKENHI (20102008). The computation in this work has been done using the facilities of the Supercomputer Center of Institute for Solid State Physics, University of Tokyo.

- 
- [1] J. Kondo, Prog. Theor. Phys. **32**, 37 (1964).
  - [2] K. Yosida, Phys. Rev. **147**, 223 (1966).
  - [3] B. Coqblin and J. R. Schrieffer, Phys. Rev. **185**, 847 (1969).
  - [4] Ph. Nozières and A. Blandin, J. Physique **41**, 193 (1980).
  - [5] B. A. Jones and C. M. Varma, Phys. Rev. Lett. **58**, 843 (1987).
  - [6] B. A. Jones *et al.*, Phys. Rev. Lett. **61**, 125 (1988).
  - [7] D. L. Cox, Phys. Rev. Lett. **59**, 1240 (1987).
  - [8] J. Kondo, Physica B+C **84**, 40 (1976); Physica B **84**, 207 (1976).
  - [9] K. Vladar and A. Zawadowski, Phys. Rev. B **28**, 1564 (1983); *ibid* **28**, 1582 (1983).
  - [10] C. C. Yu and P. W. Anderson, Phys. Rev. B **29**, 6165 (1984).
  - [11] L. G. G. V. Dias da Silva and E. Dagotto, Phys. Rev. B **79**, 155302 (2009).
  - [12] S. Yashiki *et al.*, J. Phys. Soc. Jpn. **79**, 093707 (2010).
  - [13] S. Yashiki *et al.*, J. Phys. Soc. Jpn. **80**, 064701 (2011).
  - [14] S. Yashiki and K. Ueda, J. Phys. Soc. Jpn. **80**, 084717 (2011).
  - [15] S. Sanada *et al.*, J. Phys. Soc. Jpn. **74**, 246 (2005).
  - [16] K. G. Wilson, Rev. Mod. Phys. **47**, 773 (1975).
  - [17] Since  $T_K$  is determined by the tunneling matrix element between the polaron doublet whose energy is reduced by  $U$ ,  $T_K$  is increased with the increase of  $U$ .
  - [18] In actual cage materials, we roughly estimate  $V_1$  in the order of 0.01 eV, which does not seem to be large enough to observe electric dipolar Kondo effect. However, in actuality, anharmonicity exists in the vibration. When we consider the effect of anharmonicity [14], the polaron binding energy is increased and the electric dipolar Kondo effect is expected to occur more easily.
  - [19] T. Hotta, J. Phys. Soc. Jpn. **77**, 103711 (2008).